ARCHIVES OF BIOCHEMISTRY AND BIOPHYSICS
Vol. 355, No. 2, July 15, pp. 181–188, 1998
Article No. BB980743

An Electrochemical, Kinetic, and Spectroscopic Characterization of [2Fe–2S] Vegetative and Heterocyst Ferredoxins from *Anabaena* 7120 with Mutations in the Cluster Binding Loop[1]

Anne M. Weber-Main,* John K. Hurley,† Hong Cheng,‡ Bin Xia,‡ Young Kee Chae,‡ John L. Markley,‡ Marta Martinez-Júlvez,§ Carlos Gomez-Moreno,§ Marian T. Stankovich,*,[2] and Gordon Tollin†

*Department of Chemistry, University of Minnesota, Minneapolis, Minnesota 55455; †Department of Biochemistry, University of Arizona, Tucson, Arizona 85721; ‡Department of Biochemistry, University of Wisconsin, Madison, Wisconsin 53706; §Departamento de Bioquímica y Biología Molecular y Celular, Universidad de Zaragoza, E-50009 Zaragoza, Spain

Received February 18, 1998, and in revised form May 1, 1998

Residues within the cluster binding loops of plant-type [2Fe–2S] ferredoxins are highly conserved and serve to structurally stabilize this unique region of the protein. We have investigated the influence of these residues on the thermodynamic reduction potentials and rate constants of electron transfer to ferredoxin: $NADP^+$ reductase (FNR) by characterizing various single and multiple site-specific mutants of both the vegetative (VFd) and the heterocyst (HFd) [2Fe–2S] ferredoxins from *Anabaena*. Incorporation of residues from one isoform into the polypeptide backbone of the other created hybrid mutants whose reduction potentials either were not significantly altered or were shifted, but did not reconcile the 33-mV potential difference between VFd and HFd. The reduction potential of VFd appears relatively insensitive to mutations in the binding loop, excepting nonconservative variations at position 78 (T78A/I) which resulted in ~40- to 50-mV positive shifts compared to wild type. These perturbations may be linked to the role of the T78 side chain in stabilizing an ordered water channel between the iron-sulfur cluster and the surface of the wild-type protein. While no thermodynamic barrier to electron transfer to FNR is created by these potential shifts, the electron-transfer reactivities of mutants T78A/I (as well as T48A which has a wild-type-like potential) are reduced to ~55–75% that of wild type. These studies suggest that residues 48 and 78 are involved in the pathway of electron transfer between VFd and FNR and/or that mutations at these positions induce a unique, but unproductive orientation of the two proteins within the protein–protein complex.

Key Words: **ferredoxin; ferredoxin:$NADP^+$ reductase; electron transfer; iron–sulfur; *Anabaena*.**

Two distinct [2Fe–2S] ferredoxin (Fd)[3] isoforms have been isolated from the cyanobacterium *Anabaena* 7120 (1, 2). In the photosynthetic electron transport chain, *Anabaena* vegetative Fd (VFd) serves as the terminal link to a variety of redox processes such as $NADP^+$ photoreduction, nitrate and nitrite reduction, and glutamate synthesis (3). In the anaerobic environment of specialized nitrogen-fixing cells, *Anabaena* heterocyst Fd (HFd) is the primary electron donor to the iron protein of nitrogenase under iron-replete conditions (1, 2, 4). The three-dimensional structures of both Fds have been determined at 1.7 Å resolution (5–7). The

[1] This work was supported by grants from the National Institutes of Health (DK15057 to G.T., GM29344 to M.T.S., and GM35976 to J.L.M.) and from CICYT (BIO97-0912-CO2-01 to C.G.M.).

[2] To whom correspondence and reprint requests should be addressed at 207 Pleasant Street SE, Minneapolis, MN 55455. Fax: (612) 626-7541. E-mail: stankovi@chem.umn.edu.

[3] Abbreviations used: dRf, 5-deazariboflavin; $dRfH^{\cdot}$, 5-deazariboflavin semiquinone; $E°'$, formal reduction potential; Fd, ferredoxin; FNR, ferredoxin:$NADP^+$ reductase; HFd, heterocyst ferredoxin; SHE, standard hydrogen electrode; VFd, vegetative ferredoxin; wt, wild type.

0003-9861/98 $25.00

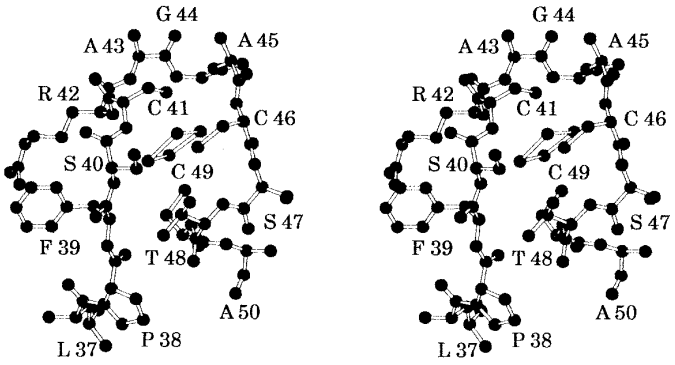

FIG. 1. Stereoview of the metal cluster binding loop of VFd, generated using the program MOLSCRIPT (33).

main chain folding patterns of these and all plant-type [2Fe–2S] Fds with known structures are highly homologous (8–12). Specifically, for *Anabaena* VFd, a majority of the 98 amino acids constituting the polypeptide chain (74%) adopt dihedral angles typical for α-helices, β-pleated sheets, and reverse turns. However, only one of the four cysteine ligands to the cluster, C49, is positioned in a standard secondary structural element. The rest of the [2Fe–2S] cluster (including cysteines 41, 46, and 79 which complete the cluster coordination sphere) is bound near the protein surface in a rather precarious binding loop composed of 13 amino acids (P38 through A50, Fig. 1) which extends nearly 9 Å away from the main body of the molecule (6).

In VFd, several interactions serve to stabilize the cluster binding loop, which would otherwise be a highly flexible region of the protein. These interactions include (i) the covalent bonds from the cysteines to the cluster irons, (ii) a salt bridge between R42 and E31, (iii) electrostatic interactions involving S64, and (iv) a series of conserved hydrogen bonds involving amino acid residues (backbone amides and/or side chain atoms) and bound water molecules (6). We have previously demonstrated that one of these hydrogen bonds (between S47 and E94) is functionally important, as nonconservative mutations at these positions result in large positive potential shifts relative to the wild-type (wt) protein ($\Delta E^{\circ\prime} = +47$ to 80 mV) and a four orders of magnitude decrease in the rate constant of electron transfer from VFd to its biological partner ferredoxin: $NADP^+$ reductase (FNR), a flavoprotein which mediates the two-electron reduction of $NADP^+$ to NADPH (13). The importance of the cluster binding loop is underscored by ^{1}H NMR studies of apoferredoxin which indicate that the apoprotein has little structure, if any. Rather, structure is induced upon cluster formation (J. L. Markley, unpublished work).

In this work, highly conserved residues located in (R42, A43, A45, T48, and A50) or near (T78) the cluster binding loop of VFd were initially targeted for site-directed mutagenesis and subsequent characterization by electrochemical, spectroscopic, and kinetic methods. Reduction potentials were determined for several VFd mutants ($E^{\circ\prime} = -384$ mV versus SHE, pH 7.5, for wt VFd (13)) to test the hypothesis that residues in this region can effectively modulate the thermodynamic redox properties of plant-type [2Fe–2S] clusters due to their close proximity to the redox-active center. These electrochemical data, while providing valuable functional information in and of themselves, were also used to select residues of interest for additional mutagenesis and kinetic studies (the latter experiments were limited in part by the availability of native FNR). Laser-flash photolysis experiments were performed on select mutants to detect perturbations in the binding of reduced Fd to oxidized FNR (K_d) and to reveal any changes in the rate constant of electron transfer within the transient (VFd_{red}:FNR_{ox}) complex (k_{et}) as per the minimal reaction scheme.

$$VFd_{red} + FNR \overset{K_d}{\rightleftharpoons} (VFd_{red}{:}FNR_{ox}) \overset{k_{et}}{\longrightarrow} VFd_{ox} + FNR_{red}. \quad [1]$$

All of the targeted residues (with the exception of A50) are capable of forming hydrogen bonds via their amide nitrogens with either the inorganic or the cysteinal sulfurs of the cluster. The choice of binding loop residues to investigate was also motivated by functional and structural differences between VFd and HFd. While its primary function is in nitrogen fixation, HFd is also 54% as active as VFd in $NADP^+$ photoreduction (14). In contrast, VFd reacts poorly with the nitrogenase iron protein. The reduction potential of HFd has been determined to be -351 mV at pH 7.5—33 mV more positive than that of VFd (13). Despite their functional differences, a comparison of the X-ray crystal structures of the proteins reveals strong similarities in their polypeptide backbones; excluding two small regions consisting of residues 9–24 and three C-terminal residues, their α-carbons superimpose with a root-mean-square deviation of 0.45 Å (6). Moreover, within the cluster binding loops of both proteins, the patterns of hydrogen bonds surrounding the [2Fe–2S] cluster are nearly identical. The proteins are 51% homologous, but have several variations in their cluster binding loops. Thus, subtle structural differences in the cluster binding region of the proteins may in part account for the functional differences between VFd and HFd. We have previously prepared a variety of single- and multiple-site hybrid mutants—formed by swapping one or more conserved binding loop residues from the sequence of one Fd to the other—and have characterized them by uv/visible and ^{15}N NMR spec-

troscopies (15). In this work, we investigate the origin of the 33-mV potential difference between VFd and HFd while evaluating the ability of specific residues to modulate the reduction potentials and/or rate of electron transfer to FNR.

MATERIALS AND METHODS

Protein preparation and mutagenesis. Wild-type vegetative and heterocyst cell *Anabaena* Fds, and their single- and multiple-site mutants, were prepared as previously described (15, 16). Native FNR for the laser-flash photolysis experiments was purified by the method of Pueyo and Gomez-Moreno (17).

Reduction potential measurements. The methodology for the determination of Fd reduction potentials by spectroelectrochemical titrations has been described (13, 18). All potentials are reported versus the SHE at the experimental conditions of pH 7.5 and 4°C. Benzylviologen and/or methylviologen (both from Sigma) were employed as indicator dyes. Typical experimental solutions contained 15–45 μM protein, 1–5 μM dye, and 1 μM 5-deazaflavin (gift of Dr. Sandro Ghisla) in 50 mM potassium phosphate buffer and 1 mM EDTA, pH 7.5, 4°C. Molar absorptivities of oxidized hybrid Fds were determined from a combination of amino acid quantitation and uv/visible spectroscopy. Molar absorptivities of reduced hybrid Fds were determined from their fully reduced spectra in electrochemical titrations. Molar absorptivities of all other Fds were assumed to be identical to that of wt VFd. Each Fd displayed Nernstian behavior based on the slopes of their Nernst plots (close to 55 mV, the theoretical slope for a one-electron transfer at 4°C).

Circular dichroism spectroscopy. CD spectra were measured in the visible and near-uv regions using an Aviv Model 60DS Spectropolarimeter (Aviv Assoc., Lakewood, NJ). Proteins were present at concentrations of 15–43 μM in H_2O and adjusted to 100 mM ionic strength with NaCl.

Laser-flash photolysis. The laser-flash photolysis system used for transient kinetic measurements (18) and the optical detection system (18–20) have been described. Electron transfer from Fd_{red} to FNR_{ox} was initiated by photochemical reaction of EDTA with the triplet state of 5-deazariboflavin (dRf) (21–23). The resulting deazariboflavin semiquinone ($dRfH^{\cdot}$) reduced Fd_{ox}, which subsequently reacted with FNR_{ox}. For the determination of pseudo-first-order rate constants, FNR (typically five to six concentrations over the range of 5–40 μM) was titrated into anaerobic buffered solutions (4 mM potassium phosphate, 1 mM EDTA, 100 mM ionic strength, pH 7.0) containing 15–43 μM wt or mutant VFd and 0.1 mM 5-deazariboflavin. The k_{et} and K_d values for the transient (Fd_{red}:FNR_{ox}) complex were calculated by fitting the saturation kinetics data to the exact solution of the differential equation describing the reaction mechanism in Eq. [1] (24, 25). These values were not corrected for the concentration of preformed (Fd_{ox}:FNR_{ox}) as described in Hurley *et al.* (26). Such a correction would result in an appreciable lowering of the K_d value, but would produce no significant change in the k_{et} value—the parameter of significance in the present study.

RESULTS AND DISCUSSION

Four single-site VFd mutants (A43S, A45S, T48S, A50N) and one quadruple mutant—in which all four mutations were incorporated into the same protein—were characterized by spectroelectrochemistry to test the functional importance of conserved residues in the cluster binding loop of plant-type Fds (Table I). The uv/visible spectra of all mutants (oxidized and reduced) were identical to that of wt VFd (data not shown).

TABLE I

Reduction Potentials of Wild-Type and Mutant VFds with Variations in the Cluster Binding Loop

Ferredoxin	$E^{\circ\prime}$[a] (mV)
wt VFd	−384[b]
A43S	−381
A45S	−375
T48S	−401
A50N	−384
A43S, A45S, T48S, A50N	−406

[a] The typical error in reduction potential measurements was ± 1–3 mV.
[b] Taken from Ref. (13).

Overall, the reduction potential of VFd was relatively insensitive to this particular set of mutations within the cluster binding loop. Of the singular mutants, only A45S and T48S induced significant shifts in potential compared to wt ($\Delta E^{\circ\prime}$ = +9 and −17 mV, respectively). These shifts are surprisingly minor for residues located within 5.0 to 8.5 Å from the cluster, compared to shifts as large as +93 mV reported for nonconservative mutations at surface residues positioned 8 to 17.5 Å from the cluster (13). The small positive shift in potential for A45S has also been observed by Vidakovic *et al.* (27). From a combination of computer modeling approaches and spectroscopic analyses (CD, EPR, and resonance Raman), they attributed the more positive potential to an additional hydrogen bond in the mutant between the hydroxyl moiety of S45 and the sulfur of the C41 cluster ligand.

Our studies show that in contrast to A45S, introduction of a serine at position 48 shifts the VFd potential negatively. Moreover, the quadruple mutant has a potential of −406 mV, which can be attributed to the negative shift induced by the single T48S mutation. A comparison of the amino acid sequences of plant-type Fds (28) and their reported reduction potentials (29) indicates that the identity of residue 48 (threonine or serine) may be partially responsible for the wide range of potentials observed in nature—with more negative potentials associated with Fds higher plants with a serine at this position versus Fds from cyanobacteria or algae with a threonine in the same location. Interestingly, in the vertebrate-type [2Fe–2S] Fd, adrenodoxin, replacement of T54 (analogous to T48 in *Anabaena*) by a serine or alanine also induces a negative potential shift (30), suggesting that this residue is directly involved in redox potential tuning in several classes of [2Fe–2S] Fds.

The influence of residue 48 on the reduction potential is not surprising in light of its structural role. The three-dimensional structure of VFd identifies T48 as

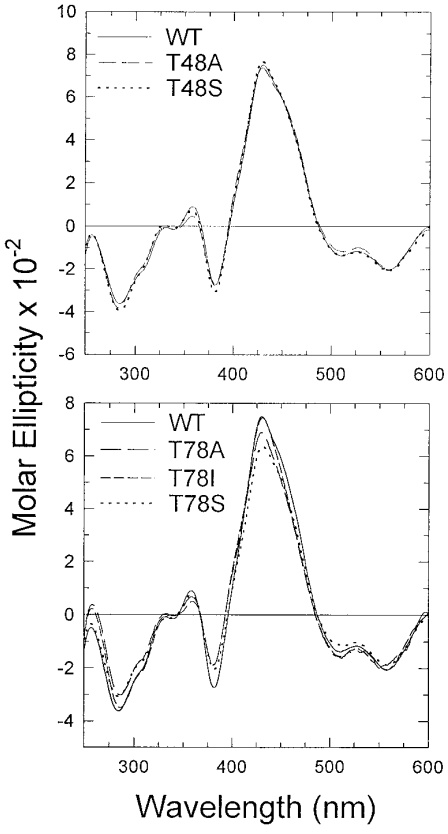

FIG. 2. Circular dichroism spectra of wt and mutant VFds. Concentrations of the Fds were as follows: wt, 43.8; T48A, 42.7; T48S, 43.3; T78A, 15.2; T78I, 35.6; and T78S, 43.0 μM. Each spectrum is an average of four scans. Other solution conditions are as given under Materials and Methods.

part of a larger evolutionarily conserved hydrogen bonding pattern which helps to stabilize the cluster binding loop by tethering it to the short C-terminal α-helix (6). Specifically, O^{γ} of T48 hydrogen bonds with S^{γ} of C46, and O of T48 hydrogen bonds with two ordered solvent molecules. In T48S, the hydroxyl moiety of the side chain is retained, as is, presumedly, its ability to form hydrogen bonds between its side chain and the C46 ligand to the cluster. Nevertheless, the diminished volume of the side chain in this mutant does appear to have a small impact on the reduction potential of the cluster. To further test the functional importance of this residue, we determined the reduction potential of the nonconservative mutant, T48A, and acquired additional optical and kinetic information for both T48A and T48S.

As shown in the top of Fig. 2, the near-uv/visible CD spectra of the oxidized T48S and T48A mutants are essentially identical to that of wt, indicating a uniformity in their protein-folding patterns and the electronic structure of their clusters. This is in contrast to the oxidized T54A mutant in adrenodoxin, whose CD spectrum reflects a rearrangement in the immediate vicinity of the cluster and whose thermal stability is decreased as a result of the mutation to alanine (30).

In the transient kinetics experiments, laser-flash excitation of the deoxygenated reaction solution containing dRf, EDTA, Fd_{ox} (wt or mutant), and FNR_{ox} results in the extraction of a hydrogen atom from EDTA by the dRf triplet state in <1 μs. This generates the deazariboflavin semiquinone which subsequently reduces Fd. The data in Table II (k_{dRfH}) show that $dRfH^{\cdot}$ reacts with T48S and T48A with a rate constant comparable to that of wt, indicating that the [2Fe–2S] cluster remains accessible and functionally active in the mutant proteins. The Fd_{red} formed in this reaction is then able to reduce FNR. For this process (see Eq. [1] for the reaction scheme), the dependence of the observed rate constant is hyperbolic as the rate-limiting step switches from complex formation to electron transfer. As shown in the top of Fig. 3, both T48S and T48A exhibit saturation kinetics. By fitting these data to the exact differential equations describing the mechanism, one can acquire values for k_{et} and the dissociation constant, K_d, of the intermediate (Fd_{red}:FNR_{ox}) complex (Table II) (24, 25). The fitted kinetic curve for T48S is indistinguishable from that for wt, and their derived k_{et} values are identical. However, T48A is only half as active as wt in electron transfer to FNR; it has a k_{et} of 3400 s^{-1} versus 6200 s^{-1} for wt. This magnitude of activity loss has been observed for Cys→Ser mutations of the cluster ligands in VFd (18) and for a variety of nonconservative mutations in acidic patches on the surface of VFd (13).

The T48A mutation leads to a decrease by a factor of 2 in k_{et}. Although this is much smaller than the decrease in k_{et} from other nonconservative mutations in the cluster binding loop (e.g., S47A, which reduces k_{et} by four orders of magnitude (13)), it nevertheless suggests that T48 plays a role in electron transfer between VFd and FNR. The K_d value for the transient electron-

TABLE II

Kinetic and Thermodynamic Parameters for Wild Type and T48 and T78 Mutants of VFd

Fd	$k_{dRfH} \times 10^{-8}$ (M^{-1} s^{-1})	k_{et} (s^{-1})	K_d (μM)	$E^{o\prime}$[a] (mV)
wt	2.0 ± 0.2	6200 ± 400[b]	9.3 ± 0.7[b]	−384[c]
T48S	1.8 ± 0.1	6200 ± 400	9.3 ± 0.7	−401
T48A	2.3 ± 0.1	3400 ± 200	8.5 ± 0.4	−382
T78S	1.9 ± 0.1	6000 ± 400	13.1 ± 1.0	−378
T78A	2.3 ± 0.1	4000 ± 300	8.4 ± 0.7	−345
T78I	1.7 ± 0.2	4400 ± 400	8.2 ± 0.7	−337

[a] The typical error in reduction potential measurements was ± 1–3 mV.
[b] Taken from Ref. (26).
[c] Taken from Ref. (13).

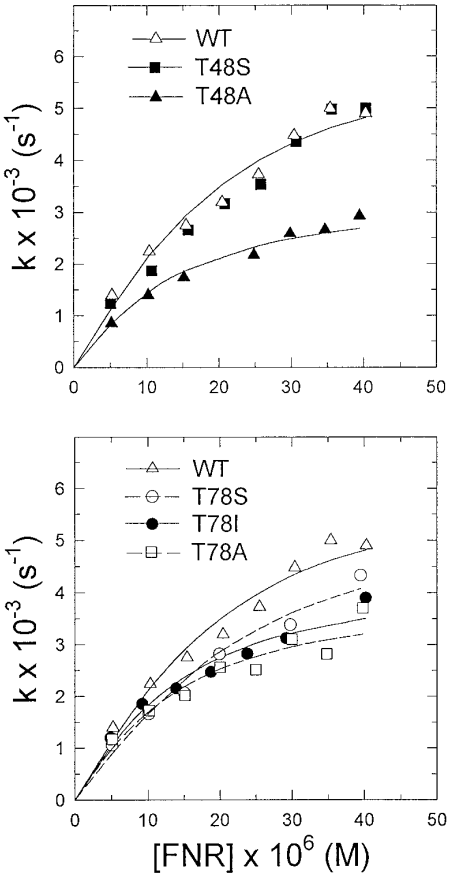

FIG. 3. Pseudo-first-order rate constants for the reduction of various concentrations of FNR by wt and mutant VFds. FNR was titrated into solutions containing 30.0 μM wt VFd, 39.6 μM T48S, 41.9 μM T48A, 43.0 μM T78S, 35.6 μM T78I, and 15.2 μM T78A. Solid lines are theoretical fits of the data assuming a two-step mechanism as described in the text. Other reaction conditions are as given under Materials and Methods. The wt data are taken from Ref. (26).

transfer complex between VFd_{red} and FNR_{ox} is not greatly affected by the T48A mutation, indicating that the mutant can form a tight complex with its biological protein partner, albeit a less productive one. Moreover, its reduction potential ($E°' = -382$ mV) is also unchanged from that of wt, ruling out any thermodynamic barrier to electron transfer to FNR (the one-electron reduction potential for the oxidized/semiquinone form of FNR is −331 mV (13)). One possible explanation for the lowered electron-transfer reactivity of T48A is that the mutation causes a subtle structural change in the Fd, forcing it to bind to FNR in a less productive orientation. Alternatively, T48 may be a critical amino acid in the biologically preferred pathway of electron transfer from the [2Fe–2S] cluster to the VFd–FNR interface. T48 occupies a position in close proximity to both the cluster and the functionally essential S47 and E94 residues. E94 is located at the surface of the molecule and is proposed to interact with basic residues on the surface of FNR in the transient electron-transfer complex (13 and references therein). A reasonable hypothesis is that the same residues which help to stabilize the cluster binding loop of VFd via a strong hydrogen bonding network also participate in a favorable pathway for electron transfer from the [2Fe–2S] cluster of VFd to the VFd–FNR interface, a pathway which is detrimentally altered by the T48A mutation.

In either case, the T48A mutation does not impact the reduction potential of the iron–sulfur cluster. This lack of correlation between reduction potentials and kinetics of interprotein electron transfer in the Fd–FNR complex has been previously observed for other Fd mutants (13, 18) and thus was not unexpected. However, recall that a small but significant shift from the baseline wt potential ($\Delta E°' = -17$ mV) was observed for the conservative T48S mutant which retains the side chain hydroxyl moeity. The near-wt potential of the nonconservative T48A mutant was surprising in this light. Additional structural information on the T48S/A mutants is required to fully explain these observations, but clearly the protein is able to structurally compensate for the T48A mutation and thus maintain its negative reduction potential, perhaps due to its ability to form other hydrogen bonds via its backbone amide group such as that with an ordered water molecule observed in the wt VFd structure. This is in striking contrast to our data for S47, only one residue away from T48, which demonstrates that the mutation from a hydroxy amino acid to an alanine shifts the potential 47 mV positively (13). Moreover, the conservative S47T mutation shifts the potential 54 mV negatively (13)—over three times the magnitude of the shift induced by the analogous T48S mutation. Thus, it appears that the hydrogen bond between the side chains of S47 and E94 plays a critical role in determining the reduction potential of the Fd, whereas that between the side chain of T48 and C46 does not.

Our studies of the cluster binding loop region were extended in the investigation of several hybrid mutants (Table III) prepared to probe the origin of the structural and functional differences between VFd and HFd. The VFd→HFd hybrids have a vegetative Fd backbone containing one or more residues from the heterocyst Fd sequence, while the HFd→VFd hybrids have a heterocyst Fd backbone containing one or more residues from the vegetative Fd sequence. The multiple mutants in the VFd→HFd hybrid series (HV, CHV) incorporate many of the single-site mutations discussed above.

The wt VFd and HFd and the various VFd/HFd hybrids listed in Table III had been previously characterized by NMR spectroscopy (15). VFd and HFd each show a different pattern of hyperfine-shifted ^{15}N NMR signals, which can be resolved in spectra of samples

TABLE III

Reduction Potentials of Wild-Type and Hybrid Fds from *Anabaena* Vegetative and Heterocyst Cells

VFd→HFd hybrids			HFd→VFd hybrids		
Fd	Mutations in hybrid	$E^{\circ\prime}$[a] (mV)	Fd	Mutations in hybrid	$E^{\circ\prime}$[a] (mV)
VFd	Wild-type vegetative	−384[b]	HFd	Wild-type heterocyst	−351[b]
R42H	R42H	−382	H42R	H42R	−361
T78L	T78L	−395	L78T	L78T	[c]
HV	R42H, A43S, A45S, T48S, A50V	−379	VH	H42R, S43A, S45A, S48T, V50A	−326
CHV	R42H, A43S, A45S, T48S, A50V, T78L	−398	CVH	H42R, S43A, S45A, S48T, V50A, L78T	−361

[a] The typical error in reduction potential measurements was ± 1–3 mV.
[b] Taken from Ref. (13).
[c] The instability of the reduced form of L78T precluded the measurement of its reduction potential.

enriched uniformly with ^{15}N. The NMR studies indicated that a single mutation in VFd (T78L) was sufficient to change the VFd pattern to that of HFd; however, the reciprocal mutation (L78T) produced little change in the HFd pattern. It was found that multiple mutations to residues found in VFd were required to change the HFd pattern of hyperfine ^{15}N signals to one resembling the VFd spectrum. The NMR results were paralleled by changes in the optical spectra of these variants. These results were interpreted in light of known differences between the rigidity of the structures of VFd (more stable, slow backbone hydrogen exchange rates) and HFd (less stable, faster backbone hydrogen exchange rates). It appears that a single mutation in VFd suffices to let the molecule relax to the HFd conformation, but that several mutations are required to convert HFd into the more rigid VFd-like conformation.

A major motivation for measuring the reduction potentials of these proteins was to determine whether they would reflect the asymmetry observed in the NMR and optical spectra. The results in Table III show that this is not the case. Rather than changing the reduction potential of VFd (−384 mV) to one similar to that of HFd (−351 mV), the T78L mutation shifted the potential in the opposite direction ($\Delta E^{\circ\prime}$ = −11 mV). The other results shown in Table III reinforce the lack of correlation between reduction potentials and spectral changes. In addition to T78L, only one other mutant of the VFd→HFd hybrid series, CHV, exhibited a significant shift in potential, and this too was in the negative direction ($\Delta E^{\circ\prime}$ = −14 mV). The −398 mV potential of CHV can likely be attributed to the single T78L mutation, since HV (identical to CHV except for lacking T78L) has a near-wt potential. Furthermore, the near-wt potential of HV suggests that the opposite potential shifts of the single-site A45S and T48S mutations (Table I) are canceled out in this multiple mutant. Similarly, the potentials of the HFd→VFd hybrids do not correlate with their optical and NMR spectral changes. The single H42R mutation does induce a small negative shift ($\Delta E^{\circ\prime}$ = −10 mV) in the direction of the VFd value; however, the expected trend of larger negative shifts for hybrids incorporating multiple mutations (VH, CVH) was not observed. In fact, the reduction potential of VH was shifted positively rather than negatively ($\Delta E^{\circ\prime}$ = +25 mV). Interestingly, this shift is overcome upon introduction of the L78T mutation in CVH. The −361 mV potential of CVH probably reflects the H42R contribution. Unfortunately, the instability of the L78T mutant precluded the measurement of its potential. Additional single-site mutants of HFd must be studied to investigate the origin of the unique VH potential (−326 mV).

While no apparent correlation exists between the spectral properties and the reduction potentials of the hybrid mutants, both data sets suggest that residue 78 has structural and functional significance. The single mutation T78L is the only change required to impart HFd spectral properties in VFd; this residue does influence the electronic properties of the [2Fe–2S] cluster, as evidenced by a negative shift in the reduction potential of T78L compared to VFd, and in HFd, the mutation L78T severely destabilizes the protein, although five additional mutations in the first half of the HFd sequence help to restore stability (see mutant CVH, Table III). To further probe the importance of this residue, threonine 78 in VFd was individually mutated to serine, isoleucine, and alanine, and the resultant mutants were characterized by spectroscopic, electrochemical, and kinetic methods.

The bottom of Fig. 2 depicts the CD spectra of these mutants and VFd. The spectra are nearly superimposable, with only minor variations. These small differences are in contrast to the strikingly unique CD features of various VFd mutants in which the cysteine cluster ligands were individually mutated to serines (18). As shown in Fig. 3 and Table II, the conservative

mutation of a threonine to a serine in T78S does not alter its reduction potential or its k_{et} of electron transfer from VFd_{red} to FNR_{ox}. The K_d for the transient (VFd_{red}:FNR_{ox}) electron-transfer complex is slightly larger for T78S, but its magnitude is within the range of those observed for all other VFd mutants studied to date in our laboratories.

Of greater interest are the kinetic and thermodynamic parameters of the T78A and T78I mutants. When T78 is mutated to alanine or isoleucine, the k_{et} decreases to 4000 and 4400 s^{-1}, respectively, compared to 6200 s^{-1} for VFd. As suggested above for T48, mutations at residue T78 may alter the preferred pathway of the electron from the cluster to the Fd–FNR interface, thereby altering k_{et}. Furthermore, the reduction potentials of the T78A/I mutants are markedly shifted from that of wt ($\Delta E°' = +39$ and $+47$ mV for T78A and T78I, respectively), though not enough to create a thermodynamic barrier to electron transfer to FNR. It is unclear why mutations of T78 to A, I (Table II), and L (Table III) lead to such varied changes in the reduction potential of VFd. All three mutations make the side chain more hydrophobic, and the mutations I and L introduce additional bulk. Remarkably, the T78I and T78L mutations shift the wt reduction potential in opposite directions. Additional structural data are required to explain this curious thermodynamic effect. Nevertheless, position 78 appears to be critically sensitive to changes (including, as evident from this case, the position of the branching of the side chain). Interestingly, in the X-ray crystal structure of VFd, the side chain of T78 participates in a hydrogen bond with one of five ordered water molecules which form a channel leading from the interior of the protein near the [2Fe–2S] cluster to the C-terminal region and the bulk solvent (6). This solvent channel is also observed in the refined structure of HFd (7). The biological significance of this channel is unknown, but it is clearly integral to the stabilization of the cluster binding loop in the *Anabaena* [2Fe–2S] Fds. Solvent accessibility of [Fe–S] clusters in proteins has been theorized to play a role in reduction potential modulation in Fds, with redox potentials expected to become increasingly positive with increasing solvent accessibility (31). Calculations have emphasized the importance of intercalated water molecules in tuning the reduction potentials of [4Fe–4S] clusters and the role of side chain groups in determining the availability of cavities for their insertion (32). This may prove to be particularly relevant in *Anabaena* VFd, in light of the unique redox properties resulting from nonconservative mutations at T78 and E94, whose side chains form hydrogen bonds with ordered water molecules near the [2Fe–2S] cluster.

In summary, the objective of this work was to characterize the electrochemical, kinetic, and spectroscopic properties of [2Fe–2S] clusters in Fd mutants with variations in and near the cluster binding loop. The pattern of optical and NMR spectroscopic changes observed previously for the family of VFd/HFd hybrids was not echoed in their pattern of reduction potentials. For the range of VFd mutants examined, only nonconservative changes at residue 78 induced large shifts (>20 mV) in the reduction potential of the [2Fe–2S] cluster. The more positive potentials of the T78A and T78I mutants may be due to perturbation of a conserved water channel. None of the mutant potentials were shifted largely enough to erect a thermodynamic barrier to electron transfer from Fd_{red} to FNR_{ox}. Nevertheless, the electron-transfer reactivities of the mutants T48A, T78A, and T78I were reduced to 55, 65, and 73% that of wt, respectively, suggesting that either (i) these residues are directly involved in the pathway of electron transfer from the [2Fe–2S] cluster to the interfacial region of the (Fd_{red}:FNR_{ox}) complex or (ii) that their mutation induces subtle yet significant changes in the conformation of the Fd—hence perturbing the electron transfer pathway within the Fd and/or forcing a less productive orientation of Fd with FNR. These results underscore the need for additional structural studies of the mutant Fds and the Fd–FNR complex. Additional studies are in progress to extend the kinetic measurements to other mutants of Fd and to create and characterize FNR mutants.

ACKNOWLEDGMENT

We extend our thanks to Dr. Hazel Holden for creating and supplying Fig. 1.

REFERENCES

1. Böhme, H., and Schrautemeier, B. (1987) *Biochim. Biophys. Acta* **891,** 1–7.
2. Schrautemeier, B., and Böhme, B. (1985) *FEBS Lett.* **184,** 304–308.
3. Knaff, D. B., and Hirasawa, M. (1991) *Biochim. Biophys. Acta* **1056,** 93–125.
4. Böhme, H., and Haselkorn, R. (1988) *Mol. Gen. Genet.* **214,** 278–285.
5. Rypniewski, W. R., Breiter, D. R., Benning, M. M., Wesenberg, G., Oh, B.-H., Markley, J. L., Rayment, I., and Holden, H. M. (1991) *Biochemistry* **30,** 4126–4131.
6. Holden, H. M., Jacobson, B. L., Hurley, J. K., Tollin, G., Oh, B.-H., Skjeldal, L., Chae, Y. K., Cheng, H., Xia, B., and Markley, J. L. (1994) *J. Bioenerg. Biomembr.* **26,** 67–88.
7. Jacobson, B. L., Chae, Y. K., Markley, J. L., Rayment, I., and Holden, H. M. (1993) *Biochemistry* **32,** 6788–6793.
8. Fukuyama, K., Ueki, N., Nakamura, H., Tsukihara, T., and Matsubara, H. (1995) *J. Biochem.* **117,** 1017–1023.
9. Tsukihara, T., Fukuyama, K., Nakamura, M., Katsube, Y., Tanaka, N., Kakudo, M., Wada, K., Hase, T., and Matsubara, H. (1981) *J. Biochem.* **90,** 1763–1773.
10. Ikemizu, S., Bando, M., Sato, T., Morimoto, Y., Tsukihara, T., and Fukuyama, K. (1994) *Acta Crystallogr.* **D50,** 167–174.

11. Tsukihara, T., Fukuyama, K., Mizushima, M., Harioka, T., Kusunoki, M., Katsube, Y., Hase, T., and Matsubara, H. (1990) *J. Mol. Biol.* **216,** 399–410.
12. Tsutsui, T., Tsukihara, T., Fukuyama, K., Katsube, Y., Hase, T., Matsubara, H., Nishikawa, Y., and Tanaka, N. (1983) *J. Biochem.* **94,** 299–302.
13. Hurley, J. K., Weber-Main, A. M., Stankovich, M. T., Benning, M. M., Thoden, J. B., Vanhooke, J. L., Holden, H. M., Chae, Y. K., Xia, B., Cheng, H., Markley, J. L., Martinez-Júlvez, M., Gomez-Moreno, C., Schmeits, J. L., and Tollin, G. (1997) *Biochemistry* **36,** 11100–11117.
14. Schmitz, S., and Böhme, H. (1995) *Biochim. Biophys. Acta* **1231,** 335–341.
15. Chae, Y. K., and Markley, J. L. (1995) *in* Photosynthesis: From Light to Biosphere (Mathis, P., Ed.), Vol. II, pp. 633–638, Kluwer Academic, Dordrecht, The Netherlands.
16. Cheng, H., Xia, B., Reed, G. H., and Markley, J. L. (1994) *Biochemistry* **33,** 3155–3164.
17. Pueyo, J. J., and Gomez-Moreno, C. (1991) *Prep. Biochem.* **21,** 191–204.
18. Hurley, J. K., Weber-Main, A. M., Hodges, A. E., Stankovich, M. T., Benning, M. M., Holden, H. M., Cheng, H., Xia, B., Markley, J. L., Genzor, C., Gomez-Moreno, C., Hafezi, R., and Tollin, G. (1997) *Biochemistry* **36,** 15109–15117.
19. Przysiecki, C. T., Bhattacharyya, A. K., Tollin, G., and Cusanovich, M. A. (1985) *J. Biol. Chem.* **260,** 1452–1458.
20. Bhattacharyya, A. K., Tollin, G., Davis, M., and Edmondson, D. E. (1983) *Biochemistry* **22,** 5270–5279.
21. Tollin, G. (1995) *J. Bioenerg. Biomembr.* **27,** 303–309.
22. Tollin, G., and Hazzard, J. H. (1991) *Arch. Biochem. Biophys.* **287,** 1–7.
23. Tollin, G., Hurley, J. K., Hazzard, J. T., and Meyer, T. (1993) *Biophys. Chem.* **48,** 259–279.
24. Simondsen, R. P., and Tollin, G. (1983) *Biochemistry* **22,** 3008–3016.
25. Simondsen, R. P., Weber, P. C., Salemme, F. R., and Tollin, G. (1982) *Biochemistry* **21,** 6366–6375.
26. Hurley, J. K., Fillat, M. F., Gomez-Moreno, C., and Tollin, G. (1996) *J. Am. Chem. Soc.* **118,** 5526–5531.
27. Vidakovic, M., Fraczkiewicz, G., Dave, B. C., Czernuszewicz, R. S., and Germanas, J. (1995) *Biochemistry* **34,** 13906–13913.
28. Matsubara, H., and Hase, T. (1983) *in* Proteins and Nucleic Acids in Plant Systematics (Jensen, U., and Fairbrothers, D. E., Eds.), pp. 168–181, Springer-Verlag, Berlin.
29. Cammack, R., Rao, K. K., Bargeron, C. P., Hutson, K. G., Andrew, P. W., and Rogers, L. J. (1977) *Biochem J.* **168,** 205–209.
30. Uhlmann, H., and Bernhardt, R. (1995) *J. Biol. Chem.* **270,** 29959–29966.
31. Stephens, P. J., Jollie, D. R., and Warshel, A. (1996) *Chem. Rev.* **96,** 2491–2513.
32. Jensen, G. M., Warshel, A., and Stephens, P. J. (1994) *Biochemistry* **33,** 10911–10924.
33. Kraulis, P. J. (1991) *J. Appl. Crystallogr.* **24,** 946–950.